This manuscript has been submitted to a peer-reviewed journal and is currently under review.

Manuscript Title: Bridging general and targeted monitoring to reduce detectability bias in population indicators in the Common Quail

Authors: Francesc Sardà-Palomera[1], Manel Puigcerver[2], Irene Peña de la Cruz[1,3], Marc Anton[4] & José Domingo Rodríguez-Teijeiro[3]

[1] Biodiversity Management and Conservation Program, Forest Science and Technology Center of Catalonia (CTFC), Solsona, Spain.

[2] Retired researcher, formerly at Universitat de Barcelona, Spain.

[3] IrBio and Departament de Biologia Evolutiva, Ecologia i Ciències Ambientals, Universitat de Barcelona, Spain.

[4]Catalan Ornithological Institute (ICO), Edifici Forum, Plaça Leonardo da Vinci 4-5, 08019 Barcelona, Catalonia, Spain.

Corresponding author: Francesc Sardà-Palomera, e-mail: francesc.sarda@ctfc.cat

Keywords: abundance estimation; biodiversity assessment; long-term monitoring; population trends; sampling bias; species-specific surveys; volunteer-based monitoring

Abstract

Breeding Bird Monitoring Schemes (BMS), a cornerstone of large-scale volunteer-based ecological monitoring, are central to biodiversity assessment and conservation decision-making. However, their generalist design means that detectability can vary across species, habitats and behavioral states, introducing noise into abundance estimates and population indices. Improving how BMS account for detectability-related bias is therefore essential for strengthening their applied value in conservation and management, particularly when population indicators are used to guide policy, prioritization and adaptive management actions. Here, we develop and test a calibration framework to adjust for detectability-related bias in BMS counts by integrating information from a targeted, species-specific high-detection survey conducted in parallel. Using the Common Quail (*Coturnix coturnix*), a farmland species whose irregular and density-dependent calling behavior generates strong variation in detectability, we quantified differences in detection, abundance estimates and temporal trends between the two monitoring approaches. The targeted survey detected quails in 32% of surveys classified as absences by the BMS method, revealing substantial detectability mismatches. When detections occurred under both methods, the targeted survey recorded more than twice as many individuals per survey, indicating marked bias in local abundance estimates under general monitoring. We then fitted a habitat-informed calibration model that adjusts BMS counts using vegetation greenness (NDVI) as a proxy of habitat quality. Discrepancies between methods were largest in high-quality habitats and under low BMS counts. Applying the calibration reduced noise associated with detectability variability and improved the reliability of BMS-derived trend indices. By explicitly addressing detectability-related bias, this approach provides an operational and transferable framework for improving monitoring-based indicators used in conservation assessment and management. More broadly, it illustrates how integrating targeted, high-detection surveys with broad-scale volunteer-based monitoring can enhance the decision relevance of biodiversity monitoring programs without compromising their scalability or long-term continuity.

INTRODUCTION

Breeding bird monitoring schemes (BMS) are the cornerstone of large-scale biodiversity assessment worldwide (Gregory et al. 2005, Likens and Lindenmayer 2018). Their standardized protocols, broad spatial coverage and long-term continuity allow robust quantification of population change and ecological responses to environmental pressures through abundance-based indicators and trend indices (e.g.: Devictor et al., 2008; Rigal et al., 2023; Stephens et al., 2016). A defining feature of these schemes is their reliance on trained volunteer observers, whose coordinated effort generates large multispecies datasets that would be unfeasible through professional surveys alone (Moussy et al. 2022). By providing consistent information across extensive temporal and geographic scales, BMS programs play a key role in informing conservation policy, land-use planning and biodiversity indicators at national and international levels (Schmeller et al. 2009, Tulloch et al. 2013). Ensuring the methodological reliability and taxonomic representativeness of these schemes is therefore essential for accurately tracking environmental change (Yoccoz et al. 2001, Kissling et al. 2018).

Despite the success of BMS, their generalist and multispecies design inevitably introduces substantial variation in detection probability across species, habitats and regions (Thompson, W.L. 2002, Diefenbach et al. 2003). Species whose behavior, spatial dynamics or social organization depart from the assumptions of standard count protocols may yield biased indicators outputs in general monitoring schemes. Such biases may arise through missed detections, ambiguous records or potential double-counting (Guillera-Arroita et al. 2017). These issues are especially problematic for species that fall outside the core “common bird” set typically covered by BMS programs, including those that are behaviorally atypical, patchily distributed or otherwise difficult to survey using standard protocols (Nichols et al. 2007, Sardà-Palomera et al. 2012a).

Biases in detection probability can propagate through population indices, affecting abundance-based indicators, temporal trends and the ability of monitoring schemes to detect true demographic change (Kéry and Schmidt 2008). When detection is variable or inconsistent, yearly indices may become distorted, trend precision decreases and interannual variability inflates, particularly when uncertain observations are unevenly distributed across space or time (Johnson 2008, Kellner and Swihart 2014). In long-term

monitoring schemes, these effects can compromise the reliability and interpretability of populations.

As a consequence of these limitations, large-scale biodiversity indicators—such as those produced by the Pan-European Common Bird Monitoring Scheme (PECBMS, Brlík et al. 2021)—typically exclude species with low or highly variable detectability, focusing instead on widespread and consistently monitored taxa (Gregory et al. 2005, 2008, Brlík et al. 2021). This exclusion avoids introducing methodological noise into continental indicators, but it also means that many ecologically relevant or management-sensitive species remain poorly represented in general monitoring outputs. To address this gap, species-specific monitoring programs have been developed by universities, research institutes and public administrations, using tailored protocols that substantially increase detectability and provide more accurate abundance estimates for species whose behavior or ecology challenge standardized monitoring (Bibby et al. 2000).

These limitations underscore the need for methodological comparisons between general BMS protocols and species-specific surveys. Such comparisons help clarify how detectability, sampling effort, observer performance and habitat structure influence indicators outputs (Johnson 2008), and they provide the basis for developing calibration approaches that improve the robustness, consistency and comparability of abundance-based indicators derived from large-scale monitoring schemes (Kellner and Swihart 2014) .

In this study, we compare indicator outputs from a BMS with those from a species-specific monitoring program for the Common Quail (*Coturnix coturnix*). The Common Quail is a widespread farmland species whose behavioral particularities—most notably its reliance on male vocal activity for detection – mean that strong context- and density-dependent variation in calling behavior may generate substantial detectability bias under standardized BMS protocols (see Section 2.1 for details). The species also holds high socioeconomic relevance due to its importance in small-game hunting (Perennou, C. 2009). Consequently, robust population indicators are essential for conservation and management, yet detectability related uncertainty remains a central point of debate in quail monitoring and harvest regulation (Arroyo et al. 2022). This uncertainty is reflected in the inconsistent treatment of the species across monitoring frameworks, with continental indicator excluding it from trend reporting, while national or regional

programs continue to publish Common quail population assessments (Brlík et al. 2021, Escandell et al. 2023, ICO 2025).

In this context, we set out to (1) quantify differences in presence–absence detection and abundance-based indicators between a general breeding bird monitoring scheme—the Catalan Common Bird Monitoring Survey (SOCC)—and a species-specific survey designed for the Common Quail (SEC), (2) develop a calibration model that translates SOCC counts into SEC-equivalent abundance indicators, and (3) assess how applying this correction influences long-term indicator trends. By developing and testing this calibration tool, we evaluate whether data from a general BMS can be adjusted to improve indicator performance for a behaviorally atypical farmland species and identify the conditions under which detectability-related biases can be mitigated.

MATERIAL AND METHODS

Study species

The Common Quail is a small migratory galliform associated with open farmland in the Western Palearctic, particularly cereal crops and other herbaceous vegetation (McGowan et al. 2020). Individuals typically remain hidden within dense cover, making visual detection uncommon. Consequently, male vocalizations constitute the primary cue for detection in the field.

However, the environmental and social factors influencing calling activity remain poorly understood. Calling behavior is further shaped by a non-territorial mating system, characterized by loose and spatially dynamic male aggregations, whose calling intensity and spatial arrangement fluctuate in response to social interactions (Rodríguez-Teijeiro et al. 1992, Rodrigo-Rueda et al. 1997, Guyomarc'h et al. 1998, Sardà-Palomera et al. 2011). This behavioral complexity makes it difficult to predict when and where males will call, contributing to variable detectability across habitats and survey conditions.

In addition to these behavioral complexities, habitat quality strongly shapes the seasonal presence and abundance of the species. Quail distribution is known to shift in response

to crop phenology and harvesting schedules, with individuals rapidly relocating as vegetation structure changes during spring and early summer (Rodríguez-Teijeiro et al. 2009). Complementing this, remote-sensing analyses have shown that vegetation greenness (NDVI) provides a reliable proxy for these habitat dynamics, with higher NDVI values associated with increased quail presence (Sardà-Palomera et al. 2012b).

This combination of cryptic behavior, socially mediated calling patterns and strong dependence on dynamic habitat conditions poses major challenges for general bird monitoring schemes, where detectability-related biases directly affect indicators outputs.

Monitoring schemes and data collection

Common Bird Monitoring Survey (SOCC)

The Catalan Common Bird Monitoring Survey (SOCC, Herrando et al. 2008) is a volunteer-based scheme in which observers conduct standardized breeding bird counts along 3-km linear walking transects. Each transect is visited twice during the breeding season (15 April–15 May and 16 May–15 June), following a common protocol regarding survey duration (2–2.5 h), time of day (first four hours after sunrise), and weather conditions (no rain, low wind and good visibility). All individual birds (including Quails) detected by song or visually within the standardized survey period are recorded.

The SOCC program was established in 2002 and currently includes 638 transects across Catalonia. In this study, we used the subset of surveys conducted between 2005 and 2025 in which the Common Quail was detected at least once (N = 205 transects; Figure 1). The starting year was selected because it coincides with the availability of spatially explicit agricultural land-use data, which allowed the identification of suitable habitat for subsequent analyses (see Section 2.3).

Common Quail Specific Survey (SEC)

The Common Quail Specific Survey (SEC; from its Catalan acronym) is a targeted monitoring protocol originally developed at the University of Barcelona to improve the accuracy of quail counts based on behavioral research and extensive field experience

with the species (Rodríguez-Teijeiro et al. 2010, Sardà-Palomera et al. 2012b). The method was designed to maximize the detection of singing males by accounting for their cryptic behavior, socially mediated calling activity and loose male aggregations. SEC surveys were conducted by trained professional personnel along predefined transects, following a structured sequence of listening stops and acoustic stimulation.

Observers moved along a fixed route and stopped at regular intervals to perform short listening sessions outside the vehicle. At each listening point, observers remained silent for 2 minutes to detect any spontaneously calling males. When spontaneous calling occurred, these males were immediately located and targeted for capture, as they provided reliable positional cues without requiring acoustic stimulation.

When no spontaneous calling was detected, observers broadcast female calls ("lure") to stimulate vocal responses from males. The playback consisted of two series of 15–20 seconds separated by short listening pauses. If males responded, their approximate locations were recorded and the observer attempted immediate capture using a hand net while continuing to use the playback device as the lure. If no response was elicited, the playback sequence was repeated 3 additional times (two series each), with 30-second listening intervals between repetitions.

At each listening point, this sequence allowed observers to: (1) activate males that were silent, (2) capture those that approached the lure, and (3) record those that continued calling but did not move toward the observer. While acoustic stimulation is intended to increase detectability and the number of males detected, capture aims to provide individual-level confirmation, allowing observers to discriminate between distinct individuals and to limit potential over-detection arising from moving individuals and repeated or socially mediated vocal responses. Captured males were held temporarily following ethical handling protocols.

At the end of the transect, all captured individuals were ringed and subsequently released at the precise point of capture. The final count for each transect consisted of the total number of males detected (captured + uncaptured), mapped at their initial detection position, with the aim of providing a high-detection reference of local abundance aligned with the behavioral characteristics of the species.

Paired sampling design for direct comparison between schemes

Between 2021 and 2025, we designed and monitored 28 dedicated SOCC transects across Catalonia, spanning a wide range of quail suitable habitat types and altitudes (38–1158 m a.s.l.) and selected to represent areas where different quail densities were known or expected based on previous monitoring (Figure 1). Transects were progressively incorporated over the study period, resulting in variable annual sampling effort and partial overlap among years, with the maximum number of active transects reached in 2024 (n = 27). All surveys were carried out during the breeding season, between 1 April and 30 June. To ensure direct comparability between SOCC and SEC data, each transect was surveyed on two consecutive days: the SOCC survey was conducted first, followed the next day by the SEC survey at the same hour of the morning, under very similar weather conditions and by the same observer, and for the same duration. This paired and standardized sampling design minimized temporal variation in male calling activity and provided a robust basis for comparing the two monitoring schemes under equivalent site, habitat and weather conditions.

Habitat and vegetation covariates

To quantify the amount and quality of suitable breeding habitat available for Common Quails along each transect and season, we combined agricultural land-use information with remotely sensed vegetation indices. First, we identified the agricultural land-use categories considered suitable for the species based on previous studies and expert knowledge. These included cereal crops, fallows, legume crops, and herbaceous dryland mosaics, which represent the primary breeding habitats for the species in Mediterranean farmland systems. All polygons corresponding to these land-use categories were extracted from two official agricultural mapping systems: SIGPAC (the national land-parcel identification system) and DUN (the Catalan annual agricultural declaration system), both of which provide georeferenced information on crop types and field boundaries for each year between 2005 and 2025. A detailed description of the selected land-use categories is provided in Supporting Information.

For each 3-km transect and year, we quantified the amount of suitable habitat within a 300-m buffer centered on the survey route. This buffer width was selected to match the

effective detection distance used in the calibration analyses. All suitable habitat polygons intersecting the buffer were merged, and the resulting area was calculated for each transect–year combination. Suitable habitat area varied substantially among transects, ranging from 45 to 171 ha, and was included as a covariate in subsequent modelling steps.

To characterize vegetation productivity and structure, we extracted the Normalized Difference Vegetation Index (NDVI) for each transect buffer using Landsat surface reflectance imagery (Landsat 5, 7, 8, and 9; 30-m resolution). NDVI was calculated for each 15-day and monthly intervals between 1 April and 30 June of each year, following cloud and shadow masking based on the QA_PIXEL band. For each interval, NDVI values were first aggregated at the pixel level using median composites, and transect-level NDVI was then obtained by spatially averaging (mean) all pixels contained within each buffered transect area. NDVI processing was conducted in Google Earth Engine (Gorelick et al. 2017). NDVI values derived from 15-day composites were unavailable for 16% of the paired surveys due to insufficient cloud-free observations, and these surveys were therefore excluded from analyses requiring habitat classification based on 15-day NDVI. In contrast, monthly NDVI metrics were available for all surveys.

To classify SOCC transects into broad habitat-quality categories, we performed a k-means clustering analysis based on three NDVI descriptors calculated for each transect: the mean NDVI during the breeding season, the within-season standard deviation, and the interannual standard deviation (see Supporting Information). These metrics respectively captured overall vegetation greenness, short-term seasonal variability, and longer-term temporal stability. All variables were standardized prior to clustering. A two-cluster solution was selected based on minimization of the within-cluster sum of squares, yielding two distinct habitat-quality groups: transects characterized by high and stable vegetation greenness (high-quality habitat) and transects with lower and/or more variable NDVI values (low-quality habitat).

Model building and projection

We developed a calibration model to relate SOCC counts to the more sensitive SEC counts, with the aim of correcting detectability biases in the general bird monitoring

scheme. For each paired SOCC–SEC survey, the SEC count was used as the reference indicator of local abundance, and its relationship with the corresponding SOCC count was modelled using a generalized linear modelling framework. SOCC counts were included as the main predictor, and both linear and quadratic forms of the SOCC term were evaluated. Habitat covariates such as suitable-habitat area and NDVI were incorporated to account for local environmental variation, and interaction terms between SOCC and NDVI were also included among the candidate formulations.

To determine the most appropriate calibration structure, we fitted a full set of candidate models combining: (1) different NDVI metrics (mean, median, and monthly or 15-day composites), (2) alternative error distributions (Poisson, negative binomial NB1 and NB2), (3) the presence or absence of zero-inflation components, (4) linear versus quadratic SOCC effects and (5) models with or without a random intercept for transect identity. Candidate models were compared using Akaike's Information Criterion (AIC), and the most parsimonious model structure was selected based on relative AIC differences. All models were inspected for residual patterns, dispersion, and potential outliers following standard diagnostic procedures. Final model performance was evaluated by assessing the agreement between predicted and observed SEC counts. In addition, the relative contribution of individual predictors was examined using ΔAIC values derived from reduced models.

After selecting the final calibration model, SOCC counts from all transects where Common Quail had been detected at least once between 2005 and 2025 were converted into SEC-equivalent abundance indicators. For each transect and year, the observed SOCC count together with the corresponding habitat covariates was entered into the calibration model, and the resulting predictions were rounded down to the nearest integer to provide calibrated abundance-based indicators reflecting SEC-level detectability.

Trend analysis

We assessed long-term population trends for both the original SOCC counts and the calibrated SEC-equivalent indicators. Annual SOCC and SEC-equivalent counts were obtained by selecting, for each transect and year, the maximum value from the two

SOCC visits, following the standard procedure used by the Catalan Institute of Ornithology (ICO) for deriving official SOCC trends.

For each dataset, we fitted TRIM log-linear models with site and time effects to estimate annual population indices and impute missing values (Van Strien et al. 2004). To obtain a single overall indicator trend, we regressed the logarithm of the TRIM-imputed annual index against time using ordinary least squares; the slope of this regression provided a measure of the average annual rate of change.

To evaluate whether trends differed across habitat quality, each transect was assigned to one of the NDVI-based habitat clusters (see Supporting Information), and the TRIM and log-linear trend analyses were repeated separately for each habitat group. Differences between the original SOCC and calibrated SEC-equivalent indices within each habitat group were formally tested using linear models in which the logarithm of the TRIM-derived annual index was modelled as a function of time (covariate), data series (SOCC vs calibrated SEC-equivalent; fixed factor), and their interaction. All analyses were conducted in R (version 4.4.2) using the rtrim package (Bogaart et al. 2020).

RESULTS

Observed detection and count differences across schemes

The paired SOCC–SEC surveys revealed clear differences in detectability between the two monitoring schemes. In 32% of paired surveys where SOCC recorded no Common Quails, the SEC protocol detected at least one calling male (mean ± SD = 4 ± 3.4), whereas the opposite pattern was rare, with SOCC detecting a single individual while SEC detected none in only one case (7%), corresponding to an isolated detection of a single calling male. Overall, presence–absence detections differed significantly between methods, with a clear asymmetry favoring SEC detections in surveys where SOCC failed (McNemar's test, $p = 0.033$).

Across all surveys, the SEC generally recorded higher numbers of calling males than the SOCC. In 71% of paired surveys, SEC detected more individuals than SOCC, while

26% yielded identical counts and only 3% (one case) resulted in higher counts under SOCC.

Consistently, SEC detected significantly more Common Quail males per survey than SOCC (paired Wilcoxon signed-rank test: $p < 0.001$), with a mean difference of 3.5 individuals per survey. On average, SOCC detected approximately 2.9 calling males per survey, whereas SEC detected approximately 6.4, corresponding to more than a twofold increase under the SEC protocol (Figure 2).

Calibration model performance

Model comparison showed that the best-performing calibration model was a negative-binomial formulation (NB1) including the 15-day mean NDVI together with linear and quadratic SOCC terms and SOCC × NDVI interactions. Models using monthly NDVI metrics, or including random intercepts or zero-inflation components, all showed substantially higher AIC values.

The final calibration model (Table 1) captured a substantial proportion of the variability in SEC counts, providing a robust basis for converting SOCC-derived counts into SEC-equivalent abundance indicators (Supplementary material S3). Standard residual diagnostics indicated no relevant overdispersion, no zero inflation and no influential outliers, confirming robust model behavior.

An AIC-based assessment of predictor contributions revealed that NDVI was the most influential variable: removing NDVI together with its interactions produced by far the largest increase in AIC ($\Delta AIC = 74.3$). The linear ($\Delta AIC = 53.5$) and quadratic ($\Delta AIC = 20.0$) components of SOCC activity also contributed substantially to model fit, indicating a non-linear relationship between SOCC and SEC counts. SOCC × NDVI interactions further improved model performance ($\Delta AIC = 8.9$), showing that the strength of the SOCC–SEC relationship varied along the NDVI gradient. In contrast, available habitat surface had no detectable effect ($\Delta AIC = -1.9$). Overall, SEC counts were primarily driven by habitat greenness and SOCC activity, with NDVI modulating both the shape and magnitude of the calibration relationship.

The magnitude of the correction predicted by the calibration model varied across the SOCC–NDVI space. The largest discrepancies between SOCC and predicted SEC-equivalent indicators occurred when SOCC counts were low and NDVI values were high, whereas predicted SEC-equivalent counts and SOCC converged under conditions of low NDVI or when SOCC counts were relatively high (≥4). These patterns reflect the structure of the fitted SOCC × NDVI interactions (Figure 3).

Population trends

Applying the calibration model to the full SOCC dataset yielded SEC-equivalent abundance indicators for all transect–year combinations with available predictor information (N = 205 transects, 2005–2025).

TRIM analyses revealed minor differences in temporal patterns between the original SOCC counts and the calibrated SEC-equivalent indicator series. Across 2005–2025, the SOCC-based population index showed a slight decline (–2.1% per year), whereas the calibrated series remained approximately stable (+0.1% per year). A joint analysis of both series indicated that the difference in long-term trends was not statistically significant (time × series: $\beta = -0.028$, $p = 0.066$), providing only weak evidence for divergence, and suggesting that, when all transects were pooled, both indices described broadly comparable overall trajectories (Figure 4A).

However, analyses stratified by NDVI-based habitat clusters revealed marked habitat-dependent differences. In transects characterized by habitat with high and stable NDVI values, the interaction between time and data series was statistically significant ($\beta = -0.047$, $p = 0.0079$). In these greener habitats, SOCC-based indices showed a clear decline (–4.51% per year), whereas the calibrated SEC-equivalent indicator series remained stable (+0.15% per year), indicating diverging temporal trajectories between the two approaches (Figure 4B).

In contrast, in transects with habitat with low or highly variable NDVI, the interaction was not statistically significant ($\beta = -0.016$, $p = 0.306$), and both SOCC and calibrated series produced similar long-term indicator trends (SOCC: –1.36% per year; SEC-equivalent: +0.29% per year). In these habitats, the two monitoring approaches yielded

401 broadly comparable temporal patterns, with limited divergence across the study period
402 (Figure 4C).

403

404 **DISCUSSION**

405

406 BMS face important challenges when applied to species characterized by behavioral or
407 ecological traits that produce high variability in detectability across space and time (e.g.
408 (Thompson, W.L. 2002, Diefenbach et al. 2003, Guillera-Arroita et al. 2017). The
409 Common Quail is a clear example of this broader class of species, as its irregular calling
410 activity, spatially dynamic male aggregations and complex mating system generate
411 presence and abundance-based indicator patterns that standard multispecies protocols
412 struggle to capture consistently. By incorporating a species-specific monitoring protocol
413 and conducting parallel surveys, we quantified the extent to which these biological traits
414 influence detectability and indicator consistency, and developed a calibration model
415 capable of correcting these biases using data from a broad-scale monitoring scheme.

416 Differences between the two methodologies were evident not only in abundance-based
417 indicators but also in basic presence–absence detection, highlighting that detectability
418 itself is a major source of divergence. Poor agreement in low-count situations suggests
419 that many individuals remain undetected when spontaneous calling activity is low, a
420 pattern common to species whose vocal behavior varies over short temporal scales
421 (Bibby et al. 2000, Sutherland 2006). Under these conditions, passive multispecies
422 surveys may fail to register a substantial fraction of individuals, whereas targeted
423 protocols using acoustic stimulation can reveal a larger proportion of the population (De
424 Rosa et al. 2022). This mechanism explains why the species-specific survey performs
425 consistently better at both presence–absence detection and abundance-based indicator
426 performance.

427 NDVI emerged as the strongest environmental predictor in the calibration model,
428 indicating that habitat greenness and phenological state strongly modulate the
429 relationship between the two monitoring schemes. Importantly, the magnitude of the
430 correction was not constant across sites: discrepancies were greatest in high-NDVI
431 habitat when the BMS protocol recorded low counts. Because NDVI varies
432 considerably among regions and years (Pettorelli et al. 2005), the degree of

underestimation in BMS data is inherently context-dependent. Accordingly, the calibration does not act as a uniform multiplier but as a habitat-mediated adjustment shaped by local vegetation dynamics. On the other hand, the lack of a detectable effect of suitable-habitat area is consistent with the fact that all paired transects were located in landscapes where quails are normally present and habitat extent was not limiting. Within this range of conditions, habitat quality—as captured by NDVI—clearly outweighed habitat quantity in determining both local abundance and detectability.

Although the calibration improves the consistency of local abundance-based indicators, it is not designed to be directly extrapolated to derive absolute population sizes at regional or higher scales without accounting for population dynamics. Common Quail males frequently undertake movements across farmland landscapes during the breeding season, tracking changes in vegetation structure, harvesting schedules and social cues (Puigcerver et al. 1989, Rodríguez-Teijeiro et al. 2009, Sardà-Palomera et al. 2012b). Recent GPS-based tracking data indicate that individuals may move not only between neighboring SOCC transects but also across wider regional, and occasionally international, distances within the same breeding period (Sardà-Palomera et al. 2025, unpublished data), highlighting the highly dynamic nature of populations over short temporal windows.

Such mobility implies open populations with substantial turnover, increasing the risk of double counting when survey data are aggregated across space and time without explicitly modelling movement and availability. Under these conditions, the local relationship between SOCC and SEC counts should be interpreted as a calibration of detectability rather than as a direct estimator of regional population totals. Nevertheless, this limitation does not preclude the use of calibrated counts for assessing temporal change or informing population indicators when embedded within appropriate analytical frameworks that explicitly consider population openness and mobility.

Additional information on movement rates, seasonal redistribution, and connectivity among breeding areas will be essential to refine such models. In the long term, integrating movement data into calibration or state-space frameworks could allow more accurate estimates at larger spatial scales. For now, however, the high mobility of the species implies that monitoring outputs should be interpreted within narrow temporal

windows and, where appropriate, at the scale of migratory flyways rather than at lower administrative units.

From a temporal perspective, the calibration refines the ability of general BMS data to describe long-term indicator trends. Although the uncorrected BMS series broadly captured the overall regional trajectory of the species, the calibrated values reduced noise associated with detectability variability and produced indices that more closely reflect true temporal dynamics. This is particularly relevant for a species whose calling behavior fluctuates across the season and whose detectability is not constant through time. By stabilizing detection-related variability, the calibration addresses a central concern in multispecies monitoring: detectability biases can propagate into long-term indices and compromise the ability of BMS programs to detect true demographic change (Kéry and Schmidt 2008, Kellner and Swihart 2014). Correcting these biases therefore directly enhances the reliability of trend indicators.

Despite these limitations, BMS remain an indispensable component of large-scale biodiversity monitoring, providing unparalleled temporal and geographic coverage that no species-specific program could realistically achieve. The challenge, therefore, is not to replace general monitoring schemes, but to complement them in ways that explicitly address detectability-related bias.

Methodologically, the calibration establishes a functional bridge between general and species-specific monitoring schemes. It leverages the extensive spatial and temporal coverage of BMS programs while embedding information from targeted surveys that maximize detectability. This integration allows general schemes to retain their logistical advantages without inheriting the full extent of their detectability biases. Beyond the present case, similar bridging approaches could be explored for other species facing detectability challenges that may require the development of specialized monitoring protocols (e.g: *Crex crex, Burhinus oedicnemus*). In several taxa, dedicated monitoring programs now incorporate passive acoustic recorders (Sugai, et al. 2018), thermal-imaging devices (Lahoz-Monfortand Magrath, 2021) or camera-trap systems (Wearn and Glover-Kapfer 2019), among others, to increase detection rates under conditions where standard BMS protocols perform poorly. Although these technologies are generally too costly or labor-intensive for broad implementation within BMS networks, they can provide high-quality reference data that enable calibration or validation of general monitoring outputs in a manner analogous to the approach demonstrated here.

Such complementary use of broad-scale and species-specific data provides a practical way to improve detection in species that are poorly sampled by standard monitoring schemes, while highlighting the remaining challenge of translating detection-based information into abundance-based indicators suitable for robust trend assessment.

Overall, our study demonstrates that general BMS data can be partially reconciled with species-specific information to improve local abundance-based indicators and indicator trend interpretation for species with highly variable detectability. By developing a calibration model grounded in paired surveys and habitat context, we provide a practical framework that addresses major sources of detectability-related bias while retaining the extensive spatial and temporal coverage of general monitoring programs. However, the calibration obtained here is necessarily context-dependent. Behavioral patterns, population dynamics, and habitat phenology may vary across regions, years or management systems, potentially altering the relationship between general and species-specific surveys. Consequently, applying this approach to other areas may require region-specific calibration analyses to identify the most appropriate model structure. Despite this, the proposed framework offers a transferable methodological basis for integrating general and specialized monitoring schemes. More broadly, our results highlight the value of combining broad-scale volunteer-based programs with targeted high-detection surveys to generate more robust and interpretable population indicators for species whose detectability is shaped by behavioral or environmental processes.

ACKNOWLEDGEMENTS

We thank the Institut Català d'Ornitologia (ICO) for providing access to SOCC data and for its long-term commitment to bird monitoring in Catalonia. We are especially grateful to the volunteer observers, as well as to the students and field assistants who contributed to data collection and field logistics. This study was funded by the Subdirecció General de Fauna Cinegètica, Caça i Pesca Continental of the Departament d'Agricultura, Ramaderia, Pesca i Alimentació (Generalitat de Catalunya). Long-term monitoring through the SOCC program is supported by the Departament de Territori of the Generalitat de Catalunya.

CONFLICT OF INTEREST STATEMENT

The authors declare no conflicts of interest.

REFERENCES

Arroyo, B., M. Fernández-Tizón, and F. Sardà-Palomera. 2022. Análisis de los datos del programa SACRE relativos a la codorniz común (Coturnix coturnix) en la España Peninsular. IREC-CTFC.

Bibby, C. J., N. D. Burgess, and Hill, D.A. 2000. Bird census techniques. Elsevier.

Bogaart, P., M. van der Loo, J. Pannekoek, and M. P. Bogaart. 2020. Package 'rtrim.' Trends and Indices for Monitoring Data.

Brlík, V., E. Šilarová, J. Škorpilová, H. Alonso, M. Anton, A. Aunins, Z. Benkö, G. Biver, M. Busch, and T. Chodkiewicz. 2021. Long-term and large-scale multispecies dataset tracking population changes of common European breeding birds. Scientific data 8:21.

De Rosa, A, Castro, I., and Marsland, S. 2022. The acoustic playback technique in avian fieldwork contexts: a systematic review and recommendations for best practice. Ibis 164.

Devictor, V., R. Julliard, D. Couvet, and F. Jiguet. 2008. Birds are tracking climate warming, but not fast enough. Proceedings. Biological sciences / The Royal Society 275:2743–8.

Diefenbach, D. R., D. W. Brauning, and J. A. Mattice. 2003. Variability in grassland bird counts related to observer differences and species detection rates. The Auk 120:1168–1179.

551 Escandell, V., S. Herrando, and S. Escudero. 2023. Tendencia de las aves en primavera.
552 Pages 78–81 SEO/BirdLife. Programas de seguimiento y grupos de trabajo de
553 SEO/BirdLife 2023. SEO/BirdLife. Madrid.
554 Gorelick, N., M. Hancher, M. Dixon, S. Ilyushchenko, D. Thau, and R. Moore. 2017.
555 Google Earth Engine: Planetary-scale geospatial analysis for everyone. Remote
556 sensing of Environment 202:18–27.
557 Gregory, R. D., A. van Strien, P. Vorisek, A. W. Gmelig Meyling, D. G. Noble, R. P. B.
558 Foppen, and D. W. Gibbons. 2005. Developing indicators for European birds.
559 Philosophical transactions of the Royal Society of London. Series B, Biological
560 sciences 360:269–288.
561 Gregory, R. D., P. Vořišek, D. G. Noble, A. Van Strien, A. Klvaňová, M. Eaton, A. W.
562 Gmelig Meyling, A. Joys, R. P. B. Foppen, and I. J. Burfield. 2008. The generation
563 and use of bird population indicators in Europe. Bird Conservation International
564 18.
565 Guillera-Arroita, G., J. J. Lahoz-Monfort, A. R. van Rooyen, A. R. Weeks, and R. Tingley.
566 2017. Dealing with false-positive and false-negative errors about species
567 occurrence at multiple levels. Methods in Ecology and Evolution 8:1081–1091.
568 Guyomarc'h, J. C., O. Combreau, M. Puigcerver, P. A. Fontoura, and N. J. Aebischer.
569 1998. Quail. Page BWP Update 2. Oxford University Press, Oxford.
570 Herrando, S., L. Brotons, J. Estrada, and V. Pedrocchi. 2008. The Catalan Common Bird
571 Survey (SOCC): a tool to estimate species population numbers:138–146.
572 ICO. 2025. Vint-i-tresè informe del Programa de Seguiment d'Ocells Comuns a
573 Catalunya (SOCC). Institut Català d'Ornitologia (IC).

574 Johnson, D. H. 2008. In defense of indices: the case of bird surveys. The Journal of
575 Wildlife Management 72:857–868.
576 Kellner, K. F., and R. K. Swihart. 2014. Accounting for imperfect detection in ecology: a
577 quantitative review. PloS one 9:e111436.
578 Kéry, M., and B. Schmidt. 2008. Imperfect detection and its consequences for
579 monitoring for conservation. Community Ecology 9:207–216.
580 Kissling, W. D., J. A. Ahumada, A. Bowser, M. Fernandez, N. Fernández, E. A. García, R. P.
581 Guralnick, N. J. Isaac, S. Kelling, and W. Los. 2018. Building essential biodiversity
582 variables (EBV s) of species distribution and abundance at a global scale.
583 Biological reviews 93:600–625.
584 Lahoz-Monfort, J.J., and Magrath, M.J.L. 2021. A comprehensive overview of
585 technologies for species and habitat monitoring and conservation. BioScience
586 71:1038-1062.
587 Likens, G., and D. Lindenmayer. 2018. Effective ecological monitoring. CSIRO publishing.
588 McGowan, P., G. Kirwan, E. de Juana, and P. Boesman. 2020. Common quail (Coturnix
589 coturnix), version 1.0. Birds of the World.
590 Moussy, C., I. J. Burfield, P. J. Stephens, Newton, A.F.E, S. H. M. Butchart, W. Sutherland,
591 R. D. Gregory, McRae, Louise, Bubb, P., Roesler, I., Ursino, C., Wu, Y., Retief, E.F.,
592 Udin, J.S., Urazaliyev, R., Sánchez-Clavijo, L.M., Lartey, E., and Donal, P.F. 2022.
593 Aquantitative global review of species population monitoring. Conservation
594 Biology 36.
595 Nichols, J. D., J. E. Hines, D. I. Mackenzie, M. E. Seamans, and R. J. Gutierrez. 2007.
596 Occupancy estimation and modeling with multiple states and state uncertainty.
597 Ecology 88:1395–1400.

598 Perennou, C., C. 2009. European Union Management Plan Common quail. Page 71.
599 European Commission.
600 Pettorelli, N., J. O. Vik, A. Mysterud, J.-M. Gaillard, C. J. Tucker, and N. C. Stenseth. 2005.
601 Using the satellite-derived NDVI to assess ecological responses to
602 environmental change. Trends in ecology & evolution 20:503–10.
603 Puigcerver, M., J. D. Rodríguez-Teijeiro, and S. Gallego. 1989. Migración y/o nomadismo
604 en la codorniz (Coturnix c. coturnix)? Etolog﷽a 1:39–45.
605 Rigal, S., V. Dakos, H. Alonso, A. Auniņš, Z. Benkő, L. Brotons, T. Chodkiewicz, P.
606 Chylarecki, E. De Carli, and J. C. Del Moral. 2023. Farmland practices are driving
607 bird population decline across Europe. Proceedings of the National Academy of
608 Sciences 120:e2216573120.
609 Rodrigo-Rueda, F. J., J. D. Rodriguez-Teijeiro, M. Puigerver, and S. Gallego. 1997. Mate
610 switching in a non-monogamous species? The case of the common quail
611 (Coturnix coturnix). Ethology 103:355–364.
612 Rodríguez-Teijeiro, J. D., M. Puigcerver, and S. Gallego. 1992. Mating strategy in the
613 European Quail (Coturnix c. coturnix) revealed by male population density and
614 sex-ratio in Catalonia (Spain). Gibier faune sauvage 9:377–386.
615 Rodríguez-Teijeiro, J. D., F. Sardà-Palomera, I. Alves, Y. Bay, A. Beça, B. Blanchy, B.
616 Borgogne, B. Bourgeon, P. Colaço, J. Gleize, A. Guerreiro, M. Maghnouj, C.
617 Rieutort, D. Roux, and M. Puigcerver. 2010. Monitoring and management of
618 common quail coturnix coturnix populations in their atlantic distribution area.
619 Ardeola 57:135–144.
620 Rodríguez-Teijeiro, J. D., F. Sardà-Palomera, J. Nadal, X. Ferrer, C. Ponz, and M.
621 Puigcerver. 2009. The effects of mowing and agricultural landscape

622 management on population movements of the common quail. Journal of
623 Biogeography 36:1891–1898.
624 Sardà-Palomera, F., L. Brotons, D. Villero, H. Sierdsema, S. E. Newson, and F. Jiguet.
625 2012a. Mapping from heterogeneous biodiversity monitoring data sources.
626 Biodiversity and Conservation 21:2927–2948.
627 Sardà-Palomera, F., M. Puigcerver, L. Brotons, and J. D. Rodríguez-Teijeiro. 2012b.
628 Modelling seasonal changes in the distribution of Common Quail Coturnix
629 coturnix in farmland landscapes using remote sensing. Ibis 154:703–713.
630 Sardà-Palomera, F., M. Puigcerver, D. Vinyoles, and J. D. D. Rodríguez-Teijeiro. 2011.
631 Exploring male and female preferences, male body condition, and pair bonds in
632 the evolution of male sexual aggregation: the case of the Common Quail (
633 Coturnix coturnix). Canadian Journal of Zoology 89:325–333.
634 Sardà-Palomera, M. Puigcerver, Moreno-Zarate, L., Santisteban, C., and Rodríguez-
635 Teijeiro, J.D. 2025. First quail (Coturnix coturnix) markings with GPS confirm
636 previous knowledge and provide new key information for its conservation.
637 Valencia.
638 Schmeller, D. S., P.-Y. Henry, R. Julliard, B. Gruber, J. Clobert, F. Dziock, S. Lengyel, P.
639 Nowicki, E. Déri, E. Budrys, T. Kull, K. Tali, B. Bauch, J. Settele, C. Van Swaay, A.
640 Kobler, V. Babij, E. Papastergiadou, and K. Henle. 2009. Advantages of
641 volunteer-based biodiversity monitoring in Europe. Conservation biology : the
642 journal of the Society for Conservation Biology 23:307–16.
643 Stephens, P. A., L. R. Mason, R. E. Green, R. D. Gregory, J. R. Sauer, J. Alison, A. Aunins,
644 L. Brotons, S. H. Butchart, and T. Campedelli. 2016. Consistent response of bird
645 populations to climate change on two continents. Science 352:84–87.

646 Sugai, L. S. M., Silva, T. S. F., Ribeiro, J. W., and Llusia, D. 2018. Terrestrial Passive
647 Acoustic Monitoring: Review and Perspectives. BioScience:15–25.
648 Sutherland, W. J. 2006. Ecological census techniques: a handbook. Cambridge
649 university press.
650 Thompson, W.L. 2002. Towards reliable bird surveys: accounting for individuals present
651 but not detected. The Auk 119:18–25.
652 Tulloch, A. I., H. P. Possingham, L. N. Joseph, J. Szabo, and T. G. Martin. 2013. Realising
653 the full potential of citizen science monitoring programs. Biological
654 Conservation 165:128–138.
655 Van Strien, A., J. Pannekoek, W. Hagemeijer, and T. Verstrael. 2004. A loglinear Poisson
656 regression method to analyse bird monitoring data. bird 482:33–39.
657 Wearn, O. R., and P. Glover-Kapfer. 2019. Snap happy: camera traps are an effective
658 sampling tool when compared with alternative methods. Royal Society open
659 science 6:181748.
660 Yoccoz, N. G., J. D. Nichols, and T. Boulinier. 2001. Monitoring of biological diversity in
661 space and time. Trends in ecology & evolution 16:446–453.
662
663

TABLES

Table 1 Summary of the negative-binomial calibration model (NB1) relating SEC counts to SOCC counts and habitat variables.

Predictor	Estimate	SE	z	p-value
Intercept	1.739	0.104	16.690	<0.001
SOCC (linear)	1.218	0.166	7.343	<0.001
SOCC² (quadratic)	–0.370	0.090	–4.125	<0.001
NDVI (15-day mean)	0.266	0.112	2.387	0.017
Habitat area (ha)	–0.034	0.087	–0.388	0.698
SOCC × NDVI	–0.499	0.146	–3.412	<0.001
SOCC² × NDVI	0.184	0.063	2.919	0.003

FIGURE CAPTIONS

Figure 1. Geographic distribution of transects used in this study across Catalonia. Blue lines show the 28 specifically designed SOCC transects monitored with both SOCC and SEC protocols between 2021 and 2025, which were used to calibrate the SOCC–SEC relationship. Green lines represent all SOCC transects where at least one Common Quail was detected between 2005 and 2025 (N = 205), for which the calibration model was applied to generate SEC-equivalent abundance-based indicators.

Figure 2. Mean number of Common Quail males detected per transect (± SD) by the SOCC and SEC protocols. Only transects with confirmed quail detection were included. Bars show mean values and error bars indicate standard deviation.

Figure 3. Predicted SEC-equivalent quail counts as a function of SOCC counts and 15-day mean NDVI, based on the final NB1 calibration model. The surface illustrates the combined non-linear effects of SOCC and habitat greenness, as well as their interaction.

Figure 4 Temporal dynamics of the population index derived from original SOCC counts (red) and from SEC-equivalent calibrated indicators (blue). Solid lines show annual TRIM indices and shaded areas represent standard errors. Dashed lines indicate the fitted log-linear trends, with annual percentage changes shown at the right of each panel. (A) All transects combined. (B) Transects within high and stable NDVI habitats. (C) Transects within low or highly variable NDVI habitats. * denotes a statistically significant difference between SOCC and SEC-equivalent trends (time × series interaction).

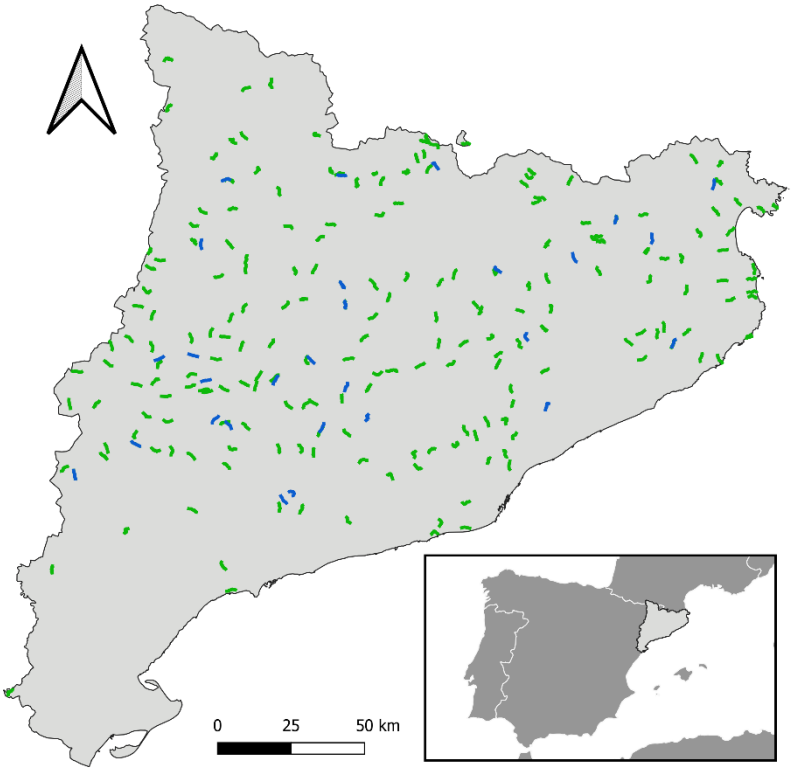

697

698 Figure 1

699

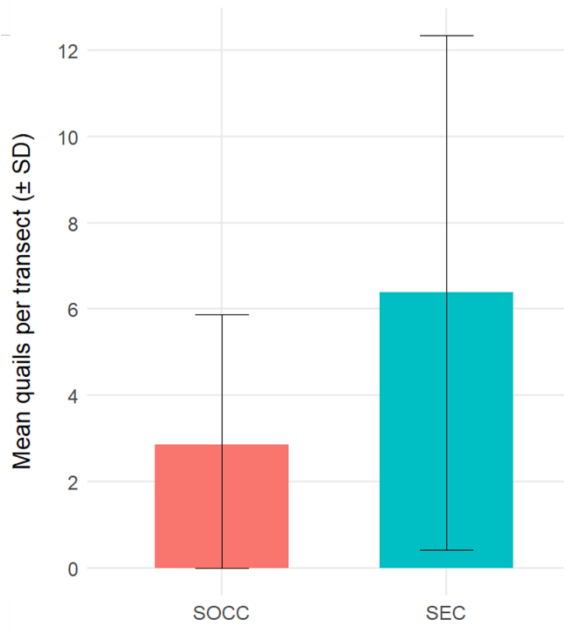

Figure 2

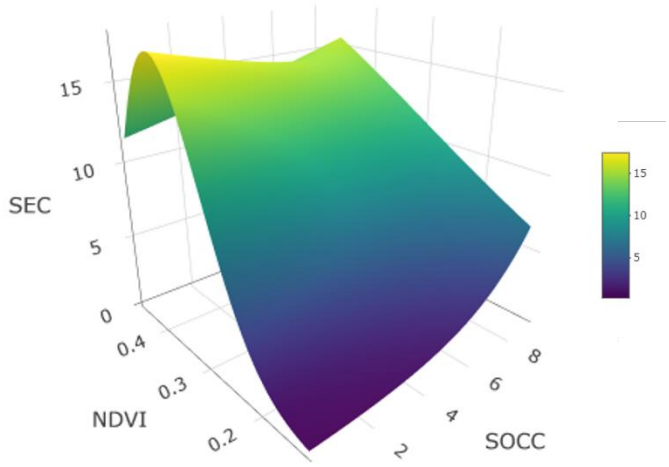

703

704 Figure 3

705

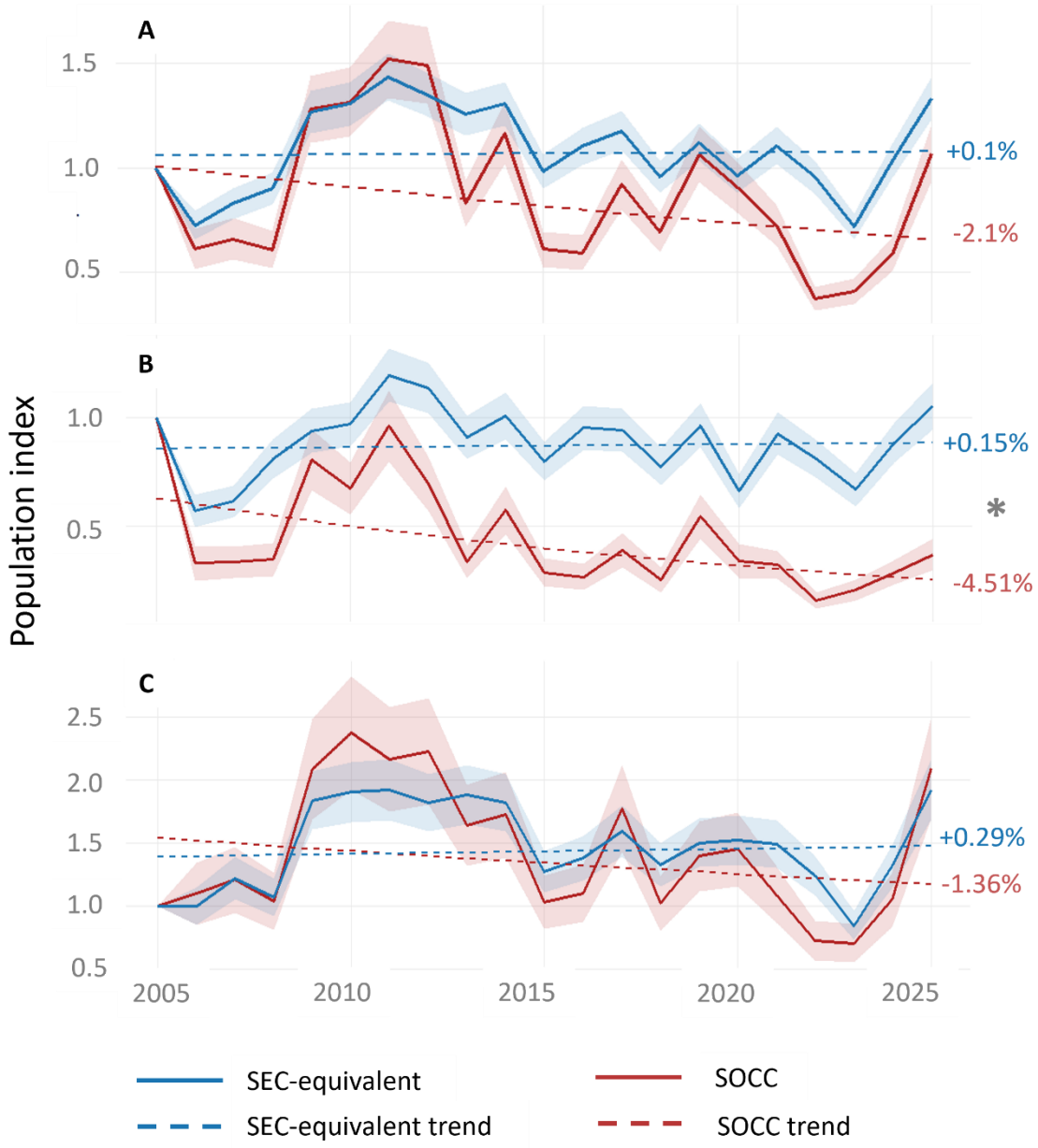

706

707 Figure 4

708

709

Supporting Information S1 – Description of agricultural land-use datasets (SIGPAC and DUN) and habitat categories used in the analyses

To classify suitable agricultural habitats for the Common Quail, we relied on two official, georeferenced land-use datasets that together cover the full study period (2005–2025):

SIGPAC (2005–2014)

The *Sistema de Información Geográfica de Parcelas Agrícolas* (SIGPAC) is the Spanish Land Parcel Identification System used for the management of the EU Common Agricultural Policy. It provides annual polygon-based information on crop type and agricultural land use at field scale. For the years **2005 to 2014**, suitable quail habitat was identified by selecting all SIGPAC polygons whose *Uso* ("TA", *Tierra Arable*) and *PS* ("Pastos") codes corresponded to cereal crops, fallows, herbaceous crops or other dryland habitats consistent with quail breeding ecology.

DUN (2015–2025)

From 2015 onwards, land-use information was obtained from the *Declaració Única Agraria* (DUN), the annual agricultural declaration system used in Catalonia and derived from SIGPAC. DUN provides detailed crop information at field level and is fully harmonised with CAP reporting requirements. For each year between 2015 and 2025, we selected all DUN polygons corresponding to herbaceous crops, cereals, legumes, fallows and other dryland herbaceous habitats considered suitable for quail breeding.

Table S1 shows the correspondence between SIGPAC and DUN crop codes

Habitat classification for modelling

All selected SIGPAC and DUN land-use categories were grouped into a single set of suitable breeding habitat types.

These habitat categories were used to:

1. calculate the area of suitable habitat within a 300-m buffer around each transect, and
2. extract vegetation indices (NDVI) for modelling quail abundance and detectability.

Table S1 provides the full lists of categories and their correspondence across datasets.

Sigpac - Suitable habitat for quail	**DUN - Suitable habitat for quail (English)**	**DUN - Suitable habitat for quail (Catalan)**
TA Arable Land	Alfalfa	ALFALS
TA Arable Land	Forage mix	BARREJA FARRATGERES
TA Arable Land	Wheat	BLAT
TA Arable Land	Chard	BLEDA
TA Arable Land	Chickpea	CIGRÓ
TA Arable Land	Oat	CIVADA
TA Arable Land	Rapeseed	COLZA
TA Arable Land	Ryegrass	ERB
TA Arable Land	Spelt	ESPELTA
TA Arable Land	Fescue	FESTUCA
TA Arable Land	Sunflower	GIRA-SOL
TA Arable Land	Fallow	GUARET
TA Arable Land	Lentil	LLENTIA
TA Arable Land	Millet	MILL
TA Arable Land	Barley	ORDI
PS Pastures	Pastures < 5 years old	PASTURES DE MENYS DE 5 ANYS
TA Arable Land	Pea	PÈSOL
TA Arable Land	Quinoa	QUINOA
TA Arable Land	Ryegrass	RAIGRAS
TA Arable Land	Rye	SÈGOL
TA Arable Land	Soybean	SOIA
TA Arable Land	Sorghum	SORGO
TA Arable Land	Sainfoin	TREPADELLA
TA Arable Land	Triticale	TRITICALE
TA Arable Land	Vetch	VEÇA

Supporting Information S2. NDVI-based habitat classification

S2.1. NDVI data processing

We characterised habitat greenness for all SOCC transects with confirmed Common Quail presence using 15-day NDVI composites derived from Landsat imagery (2005–2025). For each transect and year, we computed:

1. Annual mean NDVI: average NDVI during the breeding season.
2. Intra-annual NDVI variability: standard deviation of NDVI within the breeding season for each year.

These annual summaries were then used to derive three long-term NDVI indicators per transect:

- NDVI_mean: mean annual NDVI across all sampled years.
- NDVI_SD_intra: mean intra-annual NDVI variability.
- NDVI_SD_inter: inter-annual variability, measured as the standard deviation of annual NDVI means.
- n_years: number of years with available NDVI information.

Only transects with confirmed quail detections were retained to ensure ecologically meaningful habitat summarisation.

S2.2. Clustering analysis

To classify transects according to habitat greenness and stability, we performed k-means clustering (k = 2) on the scaled values of the three NDVI indicators:

- NDVI_mean
- NDVI_SD_intra
- NDVI_SD_inter

The number of clusters (k = 2) was selected to differentiate high-quality stable habitats from low or highly variable habitats, consistent with ecological interpretations from previous NDVI-based analyses of quail occurrence.

Cluster identities were assigned based on maximum NDVI_mean in the cluster centroids. The two habitat categories were therefore defined as:

- “NDVI high and stable” — high mean NDVI, low variability.
- “NDVI low or highly variable” — low greenness and/or high temporal fluctuation.

S2.3. Principal Component Analysis (PCA)

To validate the clustering structure, we performed a PCA using the same NDVI indicators. The first two principal components explained 46.2% (PC1) and 33.0% (PC2) of the variance, respectively.

A clear separation between the two NDVI groups was observed along PC1 (Figure S2.2), confirming that the k-means clusters captured meaningful gradients of habitat greenness and stability.

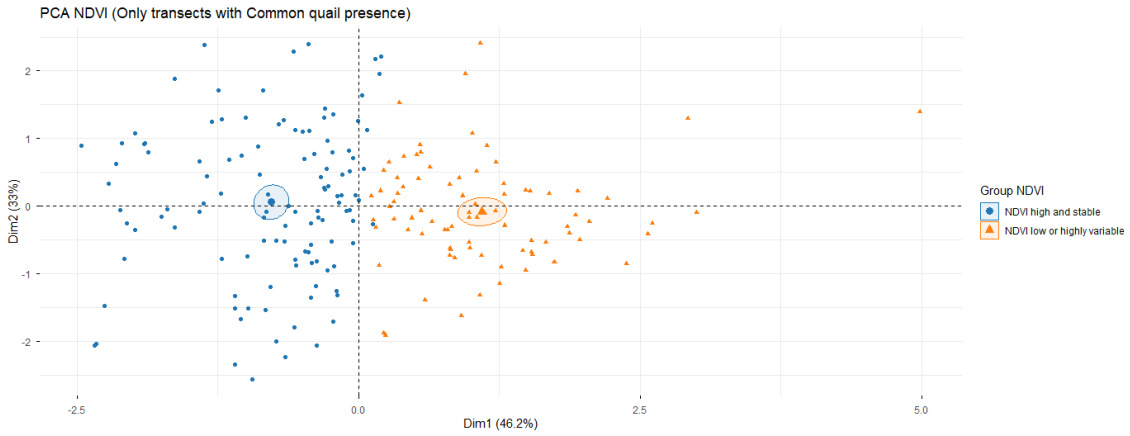

Figure S2.1. *Principal Component Analysis of NDVI indicators.* PCA of NDVI_mean, NDVI_SD_intra and NDVI_SD_inter for transects with quail presence. Colours indicate k-means habitat groups, with 95% confidence ellipses. Separation along PC1 validates the clustering structure.

S2.4. Statistical comparison of NDVI indicators between groups

To evaluate whether NDVI indicators differed significantly between habitat groups, we performed normality tests (Shapiro–Wilk) and subsequently applied either:

- Student's t-test (when both groups were normally distributed), or
- Mann–Whitney U test (for non-normal distributions).

The comparison was conducted for (Table S2.1):

- NDVI_mean
- NDVI_SD_intra
- NDVI_SD_inter

Table S2.1. Statistical comparison of NDVI indicators between habitat-quality groups. Results of parametric (t-test) and non-parametric (Mann–Whitney U) tests comparing mean NDVI, intra-annual NDVI variability and interannual NDVI variability between the two NDVI-based habitat clusters ("NDVI high and stable" vs. "NDVI low or highly variable"). Reported p-values correspond to two-tailed tests.

Variable	Test	p_value
Mean NDVI	t-test (paramètric)	< 0.001
Intra-annual NDVI SD	NDVI SD Mann–Whitney U (no paramètric)	< 0.001
Interannual NDVI SD	NDVI SD Mann–Whitney U (no paramètric)	< 0.001

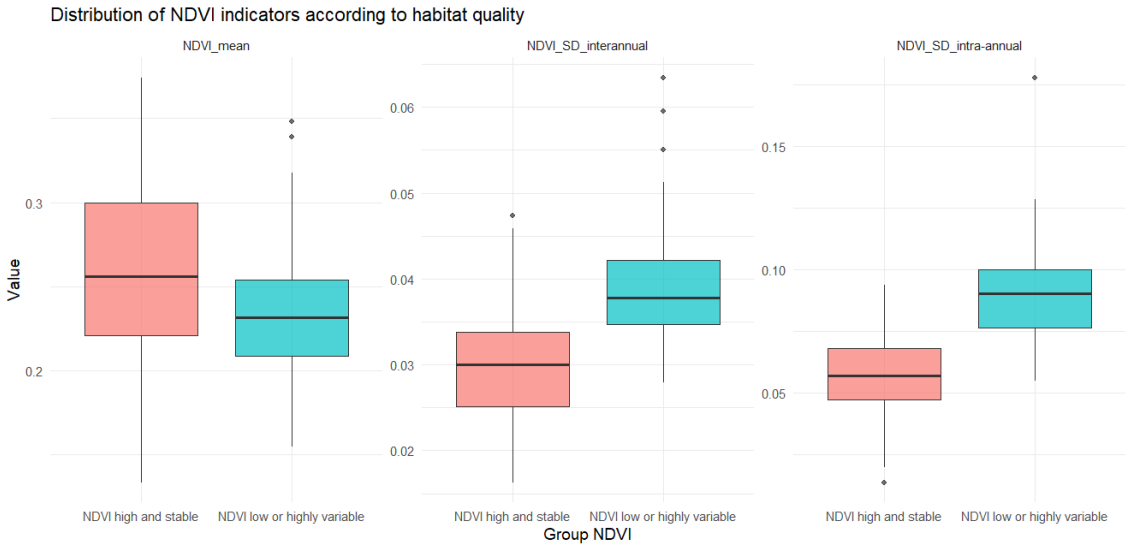

Figure S2.2. *Distribution of NDVI indicators according to habitat-quality group.* Boxplots showing (A) mean NDVI, (B) inter-annual NDVI variability, and (C) intra-annual NDVI variability for the two NDVI groups. High-NDVI stable transects show greater greenness and lower temporal variability.

Supporting Information S3 – Predictor contribution analysis

To evaluate the contribution of each predictor to the final calibration model, we compared the full model (NB1 error structure with linear and quadratic SOCC effects, 15-day mean NDVI, SOCC × NDVI interactions and suitable habitat area) with a series of reduced models in which individual terms or groups of terms were removed. Differences in Akaike Information Criterion (ΔAIC) quantify the loss of model support resulting from the removal of each component.

Table S3. Contribution of each predictor to the final calibration model based on AIC differences between the full model and models with individual terms removed.

Removed term	**df**	**AIC**	**ΔAIC**
Full model	8	282.52	0
NDVI_mean + interactions	5	356.85	74.33
socc (linear) + interaction	6	336.02	53.50
$socc^2$ + interaction	6	302.48	19.96
NDVI interactions only	6	291.45	8.93
Suitable habitat (ha)	7	280.67	–1.85

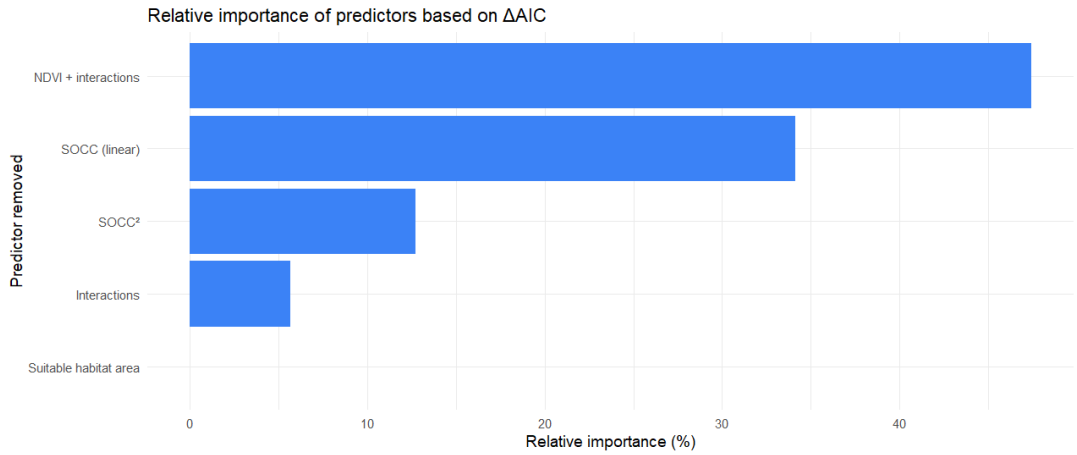

Figure S3.1. Relative importance of each predictor based on ΔAIC values obtained by removing individual terms or groups of terms from the full model. Larger ΔAIC values indicate greater loss of model support. NDVI (including interactions with SOCC) was the most influential predictor, followed by the linear and quadratic components of SOCC activity, whereas suitable habitat area had no detectable effect on indicator performance.

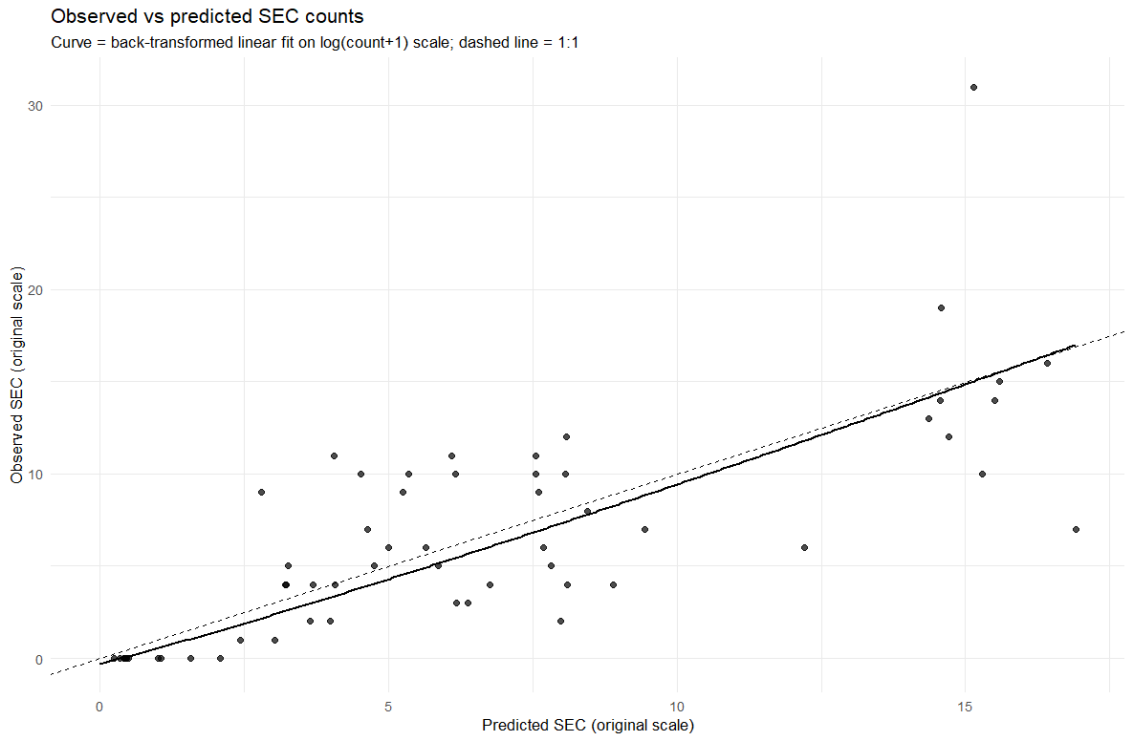

Figure S3.2. Relationship between observed and predicted SEC counts from the final calibration model (negative binomial with log link). Points are shown on the original count scale. The solid curve is the back-transformed fit from a linear regression on log(count+1), and the dashed line indicates the 1:1 relationship. Pearson correlation was computed on log(count+1) (R = 0.87).